JOC Article
pubs.acs.org/joc

Nature and Kinetic Analysis of Carbon−Carbon Bond Fragmentation Reactions of Cation Radicals Derived from SET-Oxidation of Lignin Model Compounds

Dae Won Cho,[†] Ramakrishnan Parthasarathi,[‡] Adam S. Pimentel,[†] Gabriel D. Maestas,[†] Hea Jung Park,[§] Ung Chan Yoon,*[,§] Debra Dunaway-Mariano,[†] S. Gnanakaran,[‡] Paul Langan,[‡] and Patrick S. Mariano*[,†]

[†]*Department of Chemistry and Chemical Biology, University of New Mexico, Albuquerque, New Mexico 87131,* [‡]*Bioscience Division, Los Alamos National Laboratory, Los Alamos, New Mexico 87545, and* [§]*Department of Chemistry and Chemistry Institute for Functional Materials, Pusan National University, Busan 609-735, Korea*

mariano@unm.edu

Received July 2, 2010

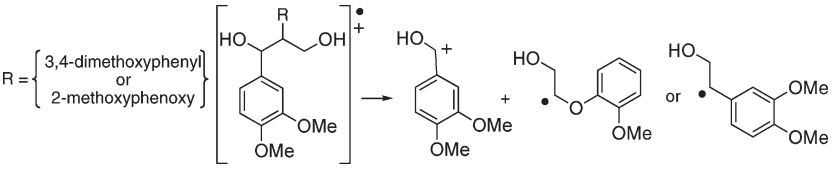

Features of the oxidative cleavage reactions of diastereomers of dimeric lignin model compounds, which are models of the major types of structural units found in the lignin backbone, were examined. Cation radicals of these substances were generated by using SET-sensitized photochemical and Ce(IV) and lignin peroxidase promoted oxidative processes, and the nature and kinetics of their C−C bond cleavage reactions were determined. The results show that significant differences exist between the rates of cation radical C1−C2 bond cleavage reactions of 1,2-diaryl-(β-1) and 1-aryl-2-aryloxy-(β-O-4) propan-1,3-diol structural units found in lignins. Specifically, under all conditions C1−C2 bond cleavage reactions of cation radicals of the β-1 models take place more rapidly than those of the β-O-4 counterparts. The results of DFT calculations on cation radicals of the model compounds show that the C1−C2 bond dissociation energies of the β-1 lignin model compounds are significantly lower than those of the β-O-4 models, providing clear evidence for the source of the rate differences.

Introduction

A major goal in the area of renewable energy research is the production of biofuels from plant biomass. If cost and energy requirements can be met, this platform will provide a CO_2-neutral method for producing combustible liquids that can be used in place of hydrocarbons. At the current time, the production of ethanol as a biofuel is based mainly on readily accessed starch found in grains. However, all plants are rich in cellulose, which through enzyme-catalyzed depolymerization can generate glucose that serves as a starting material for fermentation-based ethanol production. However, a major problem confronting this approach derives from the intimate association of the cellulose with lignin, a recalcitrant structural component of the plant cell wall.[1,2] Lignin is a complex, heterogeneous polymer biosynthesized by radical polymerization of three precursors exemplified by *p*-hydroxycinnamyl (**1**, coumaryl), 4-hydroxy-3-methoxycinnamyl (**2**, coniferyl), and 4-hydroxy-3,5-dimethoxycinnamyl (**3**, sinapyl) alcohol (Figure 1).[3,4] These components give rise to the respective *p*-hydroxyphenyl, guaiacyl, and syringyl moieties that are present in the 1,2-diarylpropanoid (β-1) and 1-aryl-2-aryloxy-propanoid (β-O-4) units in lignin (Figure 1).[5a] The β-O-4 units are predominant (ca. 55%) in the structures of most lignins, whereas the β-1 units are the second most abundant substructures (ca. 7%).[5b]

(1) Adler, E. *Wood Sci. Technol.* **1977**, *11*, 169.
(2) Radotić, K.; Micić, M.; Jeremić, M. *Ann. N.Y. Acad. Sci.* **2005**, *1048*, 215.
(3) Harkin, J. M. In *Oxidative Coupling of Phenols*; Taylor, W. I., Battersky, A. R., Eds.; Marcel Dekker: New York, 1967; pp 243−321.
(4) Brunow, G. In *Lignin and Lignin Biosynthesis*; Lewis, N. G., Sarkanen, S., Eds.; American Chemical Society: Washington, DC, 1998.

DOI: 10.1021/jo1012509 Published on Web 09/10/2010

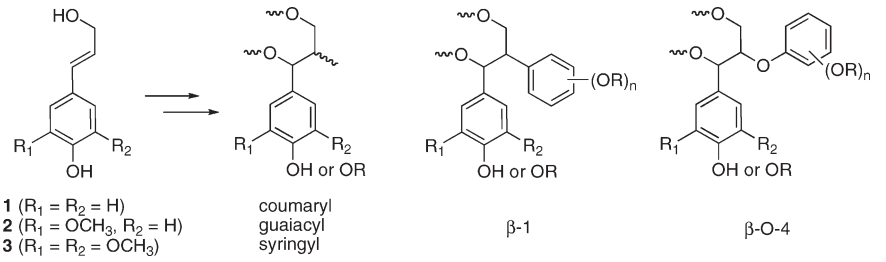

FIGURE 1. Structural units found in lignins and their biosynthetic precursors.

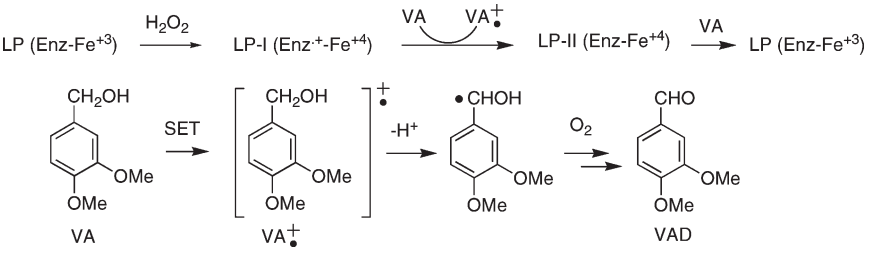

FIGURE 2. Pathway for LP-catalyzed conversion of VA to VAD.

Both the quantity and structural nature of lignins varies among plant species.[6−8] Although lignin is an essential cell wall component, it is conceivable that plants could be genetically engineered to biosynthesize a variant form of lignin that is more amenable to cost- and energy-efficient biomass batch processing. Previous work has shown that genetic manipulation of lignin biosynthetic pathway enzymes results in the production of lignin with altered composition, typically without compromise to plant growth.[9−13] Ideally, a plant variant optimized for enzyme-catalyzed lignin degradation would simplify lignin removal, which is presently achieved by costly and/or environmentally unfriendly mechanical, extractive, and/or chemical methods.

In Nature, microbes access plant cellulose using secreted enzymes ("ligninases") to catalyze lignin degradation.[5,14−18] In this regard, much attention has been given to wood-rotting fungi (e.g., *Chaetomim piluliferum* and *Phanerochaete chrysosporium*), which secrete lignin-cleaving peroxidases in combination with cellulases.[19−30] First and foremost is the iron(III) heme containing enzyme lignin peroxidase (LP), which utilizes H_2O_2 (or other oxidants) as cosubstrate.[23−25] The catalytic mechanism of LP has been examined using the H_2O_2-promoted conversion of veratrylalcohol (VA) to veratrylaldehyde (VAD) as well as other related model reactions.[31−37] Catalysis of VA oxidation follows a ping-pong mechanism wherein H_2O_2 first reacts with LP to form a doubly oxidized enzyme (LP-I) (Figure 2). VA then binds to LP-I and is oxidized by what is thought to be a single electron transfer (SET) process to produce the VA cation radical and the enzyme intermediate LP-II. The VA radical, formed by deprotonation of the cation radical, is then oxidized by molecular oxygen to form VAD. Finally, LP-II oxidizes another molecule of VA to regenerate LP.

(5) (a) Kirk, T. K.; Farrell, R. L. *Annu. Rev. Microbiol.* **1987**, *41*, 465. (b) It has been shown recently[5c] that the b-1 units in lignin exist predominantly in spirodienone forms and that these moieties are transformed to the 1,2-diarlypropan-1,3-diol forms under mild aqueous conditions.[5d] (c) Zhang, L.; Gellerstedt, G.; Ralph, J.; Lu, F. *J. Wood Chem. Technol.* **2006**, *26*, 65. (d) Lundquist, K.; Miksche, G. E. *Tetrahedron Lett.* **1965**, 2131.
(6) Grabber, J. H. *Crop Sci.* **2005**, *45*, 820.
(7) Chen, F.; Fukushima, K.; Yasuda, S. 48th Meeting of the Japan Wood Research Society, Shizuoka, Japan, **1998**, 397.
(8) Chen, F.; Yasuda, S.; Fukushima, K. *Planta* **1999**, *207*, 597.
(9) Hu, W. J.; Kawaoka, A.; Tsai, C. J.; Lung, J.; Osakabe, K.; Ebinuma, H.; Chiang, V. L. *Proc. Natl. Acad. Sci. U.S.A.* **1998**, *95*, 5407.
(10) Tsai, C. J.; Podila, G. K.; Chiang, V. L. *Plant Cell Rep.* **1994**, *14*, 94.
(11) Meyer, K.; Cusamano, J. C.; Sammerville, C.; Chapple, C. *Proc. Natl. Acad. Sci. U.S.A.* **1998**, *95*, 6619.
(12) Ralph, J.; Kim, H.; Peng, J.; Lu, F. *Org. Lett.* **1999**, *1*, 323.
(13) Ralph, J.; MacKay, J. J.; Hatfield, R. D.; O'Malley, D. M.; Whetten, R. W. *Science* **1997**, *277*, 235.
(14) Cacchio, P.; Ercole, C.; Veglio, F.; Lepidi, A. *Ann. Microbiol.* **2001**, *51*, 215.
(15) Blumer-Schuette, S. E.; Kataeva, I.; Westpheling, J.; Adams, M. W.; Kelly, R. M. *Curr. Opini. Biotechnol.* **2008**, *19*, 210.
(16) Geib, S. M.; Filley, T. R.; Hatcher, P. G.; Hoover, K.; Carlson, J. E.; Jimenez-Gasco, M. dM.; Nakagawa-Izumi, A.; Sleighter, R. L.; Tien, M. *Proc. Natl. Acad. Sci. U.S.A.* **2008**, *105*, 12932.
(17) Yang, Q.; Zhan, H.; Wang, S.; Fu, S.; Li, K. *BioResources* **2007**, *2* (4), 682.
(18) Pillinger, J. M.; Gilmour, I.; Ridge, I. *J. Chem. Ecol.* **1995**, *21*, 1113.
(19) Kuwahara, M.; Glenn, J. K.; Morgan, M. A.; Gold, M. H. *FEBS Lett.* **1984**, *169*, 247.
(20) Glenn, J. K.; Gold, M. H. *Arch. Biochem. Biophys.* **1985**, *242*, 329.
(21) Renganathan, V.; Gold, M. H. *Biochemistry* **1986**, *25*, 1626.
(22) Paszcynski, A.; Hyunh, V. B.; Crawford, R. L. *FEMS Microbiol. Lett.* **1985**, *29*, 37.
(23) Tien, M.; Kirk, T. K. *Proc. Natl. Acad. Sci. U.S.A.* **1984**, *81*, 2280.
(24) Tien, M.; Kirk, T. K. *Science* **1983**, *221*, 661.
(25) Gold, M. H.; Glenn, J. K.; Mayfield, M. B.; Morgan, M. A.; Kutsuki, H. In *Recent Advances in Lignin Biodegradation Research*; Tokyo University: Tokyo, 1983; pp 219−239.
(26) Kirk, T. K.; Farrell, R. L. *Annu. Rev. Microbiol.* **1987**, *41*, 465.
(27) Edwards, S. L.; Raag, R.; Wariishi, H.; Gold, M. H. *Proc. Natl. Acad. Sci. U.S.A.* **1993**, *90*, 750.
(28) Poulos, T. L.; Edwards, S. L.; Warishi, H.; Gold, M. H. *J. Biol. Chem.* **1993**, *268*, 4429.
(29) Poulos, T. L. *J. Biol. Chem.* **1997**, *272*, 17574.
(30) Khindaria, A.; Yamazaki, I.; Aust, S. D. *Biochemistry* **1996**, *35*, 6418.
(31) Harvey, P. J.; Schoemaker, H. E.; Bowen, R. M.; Palmer, J. M. *FEBS Lett.* **1985**, *183*, 13.
(32) Tien, M.; Kirk, T. K.; Bull, C.; Fee, J. A. *J. Biol. Chem.* **1986**, *261*, 1687.
(33) Haemmerli, S. D.; Schoemaker, H. E.; Schmidt, H. W. H.; Leisola, M. S. A. *FEBS Lett.* **1987**, *220*, 149.
(34) Marquez, L.; Wariishi, H.; Dunford, H. B.; Gold, M. H. *J. Biol. Chem.* **1988**, *263*, 10549.
(35) Andrawis, A.; Johnson, K. A.; Tien, M. *J. Biol. Chem.* **1988**, *263*, 1195–1198.
(36) Schmidt, H. W.; Haemmerli, S. D.; Schoemaker, H. E.; Leisola, M. S. *Biochemistry* **1989**, *28*, 1776.
(37) Khindaria, A.; Grover, T. A.; Aust, S. D. *Biochemistry* **1995**, *34*, 16860.

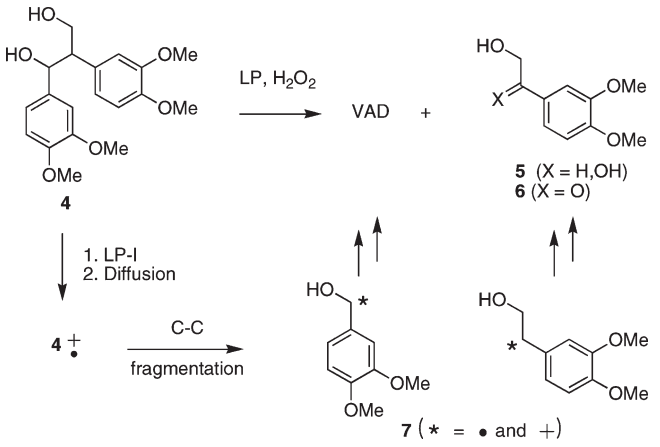

FIGURE 3. Proposed mechanism for oxidative cleavage of the lignin β-1 model **4**.

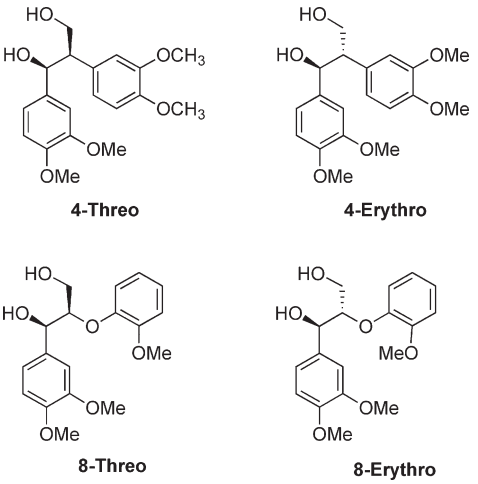

FIGURE 4. Structures of the lignin model compounds.

The detailed pathway by which LP promotes degradative cleavage of lignin is believed to involve steps that are similar to those for VA oxidation. Much of the information gained about this process derives from studies with dimeric model compounds that represent the two major structural units (β-1 and β-O-4) found in the natural polymers.[38−45] For example, LP/H_2O_2-promoted reaction of the β-1 dimeric model **4** (Figure 3) produces veratrylaldehyde mainly, along with varying amounts of the diol **5** and ketol **6**.[23] It has been proposed that the pathway involves C1−C2 bond cleavage of the 1,2-diarylethane moiety in the key cation radical intermediate formed by SET from **4** to LP-I. This process generates a cation radical pair **7**, from which deprotonation and further oxidation lead to VAD, **5**, and **6**.

The results of *in vitro* studies show that LP from *Phanerochaete chrysosporium* promotes C−C bond cleavage reactions of intact lignins that produce aldehyde-containing products, which have molecular weight distributions lower than that of the starting polymer.[46−49] In addition, kinetic analysis of interactions between LP and a oligomeric model lignin compound, carried out by Johjima and his co-workers,[47] suggests that the process involves reversible formation of a modestly tight (K_i = 330 μM) lignin LP-I complex, which undergoes conversion to LP-II (and presumably a lignin cation radical).

The observations made thus far indicate that the action of wood-rotting fungi is associated with LP-promoted C−C bond cleavage reactions of lignin; however, the actual pathway by which LP acts on lignin contained in plant cell walls has not been established. A direct pathway in which the LP makes contact with the lignin does not seem possible owing to the physical barrier imposed by the cell wall.[49] Thus, an alternative pathway involving mediation by "electron hole carriers" (mediators) has been suggested for LP delignification. Evidence to support the mediator proposal was gained in studies that showed that the presence of VA a secondary metabolite formed in *P. chrysosporium* and other methoxylated arenes lead to enhanced rates of LP-catalyzed cleavage reactions of dimeric lignin model compounds.[50,51] In addition, the reduction potential (+1.36 V, vs NHE) and lifetime ($t_{1/2}$ = 0.04 s)[52] of the VA cation radical are consistent with its possible role as a mediator in enzymatic delignification. It should be noted that alternative explanations have been suggested for the lignin cleavage enhancement effect of VA. Accordingly, VA's role might be to promote conversion of LP-II to the native enzyme[53−55] by SET and/or to protect the enzyme against degradation by excess H_2O_2.[56]

Despite their relevance to the production of ethanol from plant materials, two key aspects of radical cation promoted lignin degradation have not yet been explored. These involve the rates of the C−C bond cleavage reactions at β-1 versus β-O-4 sites and the ring substituent (alkoxy and hydroxy) effects on the C−C bond cleavage rates. Information gained from studies that probe these reactivity issues could potentially aid the genetic design of plants that have lignins that

(38) Hammel, K. E.; Tien, M.; Kalyanaraman, B.; Kirk, T. K. *J. Biol. Chem.* **1985**, *260*, 8348.
(39) Kirk, T. K.; Tien, M.; Kersten, P. J.; Mozuch, M. D. *Biochem. J.* **1986**, *236*, 279.
(40) Bono, J. -J.; Goulas, P.; Boe, J. -F.; Portet, N.; Seris, J. -L. *Eur. J. Biochem.* **1990**, *192*, 189.
(41) Hatakka, A. I.; Lundell, T. K.; Tervilä-Wilo, A. L. M.; Brunow, G. *Appl. Microbiol. Biotechnol.* **1991**, *36*, 270.
(42) Nogueira, R. F. P.; Pilli, R. A.; Durán, N. *Appl. Biochem. Biotechnol.* **1992**, *33*, 169.
(43) Lundell, T.; Wever, R.; Floris, R.; Harvey, P.; Hatakka, A.; Brunow, G.; Schoemaker, H. *Eur. J. Biochem.* **1993**, *211*, 391.
(44) Baciocchi, E.; Fabbri, C.; Lanzalunga, O. *J. Org. Chem.* **2003**, *68*, 9061.
(45) Bohlin, C.; Persson, P.; Gorton, L.; Lundquist, K.; Jönsson, L. J. *J. Mol. Catal. B: Enzym.* **2005**, *35*, 100.
(46) Hammel, K. E.; Jensen, K. A., Jr.; Mozuch, M. D.; Landucci, L. L.; Tien, M.; Pease, E. A. *J. Biol. Chem.* **1993**, *268*, 12274.
(47) Johjima, T.; Itoh, N.; Kabuto, M.; Tokimura, F.; Nakagawa, T.; Wariishi, H.; Tanaka, H. *Proc. Natl. Acad. Sci. U.S.A.* **1999**, *96*, 1989.
(48) Martinez, A. T.; Speranza, M.; Ruiz-Dueñas, F. J.; Ferreira, P.; Camarero, S.; Gullién, F.; Martinez, M. J.; Gutiérrez, A.; del Rio, J. C. *Int. Microbiol.* **2005**, *8* (3), 195.
(49) Flournoy, D. S.; Paul, J. A.; Kirk, T. K; Highley, T. L. *Holzforschung* **1993**, *47*, 297.
(50) Harvey, P. J.; Shoemaker, H. E.; Palmer, J. M. *FEBS Lett.* **1986**, *195*, 242.
(51) Baciocchi, E.; Gerini, M. F.; Lanzalunga, O.; Mancinelli, S. *Tetrahedron* **2002**, *58*, 8087.
(52) Baciocchi, E.; Bietti, M.; Gerini, M. F.; Lazalunga, O. *Biochem. Biophys. Res. Commun.* **2002**, *293*, 832.
(53) Koduri, R. S.; Tien, M. *Biochemistry* **1994**, *33*, 4225.
(54) Gilardi, G.; Harvey, P. J.; Cass, A. E.; Palmer, J. M. *Biochim. Biophys. Acta* **1990**, *1041*, 129.
(55) Haemmerli, S. D.; Leisola, M. S.; Fiechter, A. *FEMS Microbiol. Lett.* **1986**, *35*, 33.
(56) Valli, K.; Wariishi, H.; Gold, M. H. *Biochemistry* **1990**, *29*, 8535.

SCHEME 1

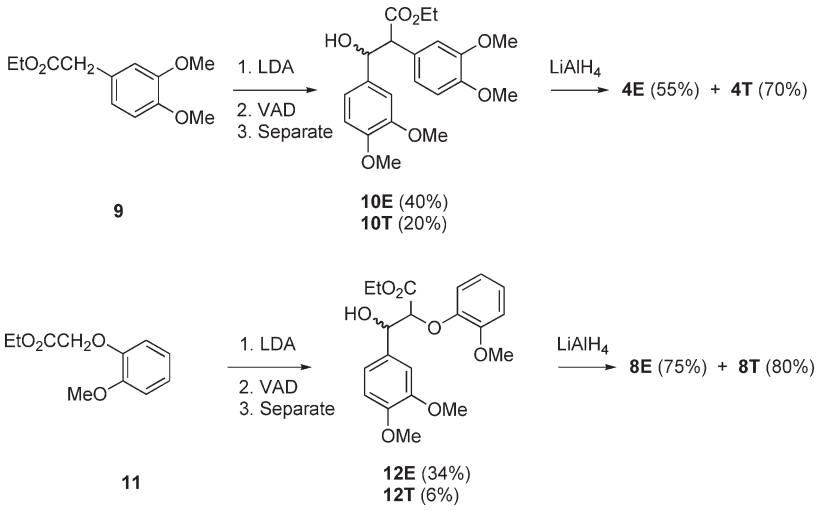

are optimized for LP or chemical oxidant based degradation (see below).

In the present work, we have addressed one important question about lignin cation radical C−C bond cleavage reactivity by exploring SET-sensitized photochemical, Ce(IV)-promoted, and LP-promoted oxidative reactions of diastereomeric dimeric lignin β-1 (**4**) and β-O-4 (**8**) model compounds (Figure 4). Kinetic analyses of these reactions show that significant differences exist in the cation radical reactivity, with the β-1 models undergoing cleavage more rapidly than the β-O-4 compounds. The results of density functional theory (DFT) calculations indicate that the β-1 cation radicals have lower bond dissociation energies than do their β-O-4 counterparts. The results of this effort are described and discussed below.

Results

Synthesis of the Lignin Model Compounds. Diastereomerically pure *erythro* and *threo* isomers of the lignin model compounds **4** and **8** were prepared by using modifications of previously reported methodologies[57] (see Supporting Information). The preparative sequences (Scheme 1) involve aldol condensation reactions of the 2-aryl- and 2-aryloxy-acetates **9** and **11** with veratrylaldehyde (VAD), followed by separation and $LiAlH_4$ reduction (Supporting Information).

SCHEME 2

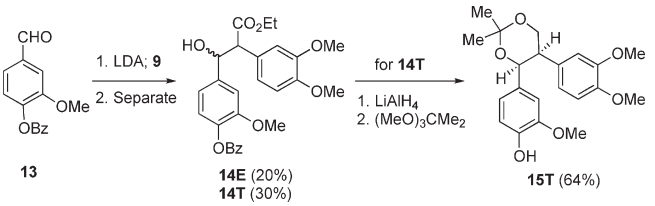

Stereochemical assignments to the *erythro* and *threo* isomers of the β-O-4 compounds, **8E** and **8T**, were made earlier[58] by using X-ray crystallographic analysis of the β-hydroxy ester **12E**, which serves as an intermediate in the synthetic route for **8E**. To assign the stereochemistry of the diastereomers of the β-1 models **4E** and **4T** (stereochemical designations of the diastereomers follows the pattern used earlier[58] for the β-O-4 compounds), the diastereomerically pure *threo* isomer of the benzoate ester **14T** was generated by condensation of acetate **9** with the veratrylaldehyde derivative **13** (Scheme 2). This substance possesses NMR spectroscopic properties that are nearly identical to those of **10T** and different from those of **10E**, the last intermediates in the synthetic routes to **4T** and **4E**, respectively. Reaction of **14T** with $LiAlH_4$ followed by acetonide formation yields **15T**, which by using X-ray crystallographic analysis (Supporting Information) was shown to possess *threo* stereochemistry.

SET-Photochemical Reactions of the Lignin Model Compounds. To determine the nature of the pathways followed in reactions of cation radical intermediates, the diastereomeric β-O-4 and β-1 lignin model compounds were subjected to SET-promoted photochemical reactions using 9,10-dicyanoanthracene (DCA) as the excited state electron acceptor (Supporting Information). DCA is ideal in this regard because (1) it absorbs light at longer wavelengths (> 350 nm) than do the lignin models **4** and **8** (λ_{max} ca. 280 nm), (2) it has a large singlet excited state reduction potential (ca. +2.8 V, vs SCE) and a relatively long singlet lifetime (ca. 15 ns), and (3) the anion radical formed from DCA by SET is reasonably stable. Irradiation (λ > 330 nm) of 5% aqueous MeCN solutions containing DCA (0.27 mM) and the *erythro* and *threo* isomers of **8** (2.1 mM) leads to formation of veratrylaldehyde (VAD), guaiacol **16**, and the independently prepared

(57) (a) Lundquist, K.; Remmerth, S. *Acta Chem. Scand.* **1975**, *B29*, 276. (b) Berndtsson, I.; Lundquist, K. *Acta Chem. Scand.* **1977**, *B31* (8), 725. (c) Ibrahim., W.; Lundquist, K.; Paulsson, M. *Acta Chem. Scand.* **1994**, *48* (2), 149. (d) Li, S.; Lundquist, K.; Maulsson, M. *Acta Chem. Scand.* **1995**, *49*, 623. (e) Miksche, G. E.; Gratzl, J.; Fried-Matzka, M. *Acta Chem. Scand.* **1966**, *20* (4), 1038. (f) Pearl, I. A.; Gratzl, J. *J. Org. Chem.* **1962**, *27* (6), 2111. (g) Pardini, V. L.; Smith, C. Z.; Utley, J. H. P.; Vargas, R. R.; Viertler, H. *J. Org. Chem.* **991**, *56* (26), 7305. (h) DiCosimo, R.; Szabo, H.-C. *J. Org. Chem.* **1988**, *53* (8), 1673. (i) Crestini, C.; D'Auria, M. *Tetrahedron* **1997**, *53* (23), 7877. (j) Nakatsubo, F.; Sato, K.; Higuchi, T. *Holzforschung* **1975**, *29*, 165. (k) Aoyama, T.; Eguchi, T.; Oshima, T.; Kakinuma, K. *J. Chem. Soc., Perkin Trans. 1* **1995**, 1905. (l) Nakata, T.; Oishi, T. *Tetrahedron Lett.* **1980**, *21* (17), 1641. (m) Stomberg, R.; Lundquist, K. *Acta Chem. Scand.* **1986**, *A40* (10), 705. (n) Li, S.; Lundquist, K.; Stomberg, R. *Acta Chem. Scand.* **1993**, *47* (9), 867. (o) Li, S.; Lundquist, K.; Soubbotin, N. *Holzforschung* **1994**, *48* (6), 509. (p) Brezny, R.; Pufflerova, A. *Collect. Czech. Chem. Commun.* **1978**, *43* (12), 3263. (q) Kovacik, V.; Mihalov, V.; Brenzny, R. *Cell Chem. Technol.* **1980**, *14* (2), 233. (r) Li, S.; Karlsson, O.; Lundquist, K.; Stomberg, R. *Acta Chem. Scand.* **1997**, *51*, 431.

(58) Langer, V.; Lundquist, K. *Acta Crystallogr., Sect. E: Struct Rep. Online* **2002**, *E58* (4), 433. Stomberg, R.; Lundquist, K. *Nord. Pulp Paper Res. J.* **1994**, *9* (1), 37.

SCHEME 3

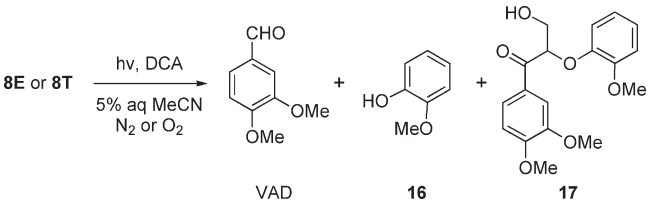

TABLE 1. Products and Yields of DCA-Promoted Photoreactions of the Lignin Model Compounds

			percent yields[c]					
substrate	conditions[a]	% conv[b]	VAD	**5**	**6**	**16**	**17**	**18**
4T	N_2 satd	52	44 (85)	8 (15)	14 (27)			4 (8)
4T	O_2 satd	100	95	trace	28			
4E	N_2 satd	46	40 (87)	4 (9)	7 (15)			trace
4E	O_2 satd	100	96	trace	40			
8E	N_2 satd	5	4 (80)			trace		
8E	O_2 satd	88	45 (51)			3	4 (5)	
8T	N_2 satd	5	4 (80)			trace		
8T	O_2 satd	90	55 (61)			5 (6)	20 (22)	

[a]Irradiation, using uranium glass filtered light, of 5% aq MeCN solutions of DCA (0.27 mM) and substrate (2.1 mM) saturated with either N_2 or O_2 for 7 h at 25 °C. [b]Based on recovered starting substrates, determined by HPLC analysis. [c]Yields based on recovered starting materials, determined by using HPLC.

(Supporting Information) keto-alcohol **17** (Scheme 3) in the yields given in Table 1.

As can be seen by viewing the data given in Table 1, the extent of conversion of the substrates for fixed time irradiations is significantly enhanced in DCA-promoted photoreactions occurring on oxygen-saturated solutions of the diastereomers of **8**. In addition, reactions of **8E** and **8T** in the presence of O_2 take place with similar chemical efficiencies but produce different ratios of VAD and keto-alcohol **17** (i.e., VAD:**17** from **8E** = 10:1 and from **8T** = 3:1).

DCA-induced photoreactions of the β-1 model compounds **4T** and **4E** take place more efficiently (as determined qualitatively by comparing irradiation times vs conversions) than those of the β-O-4 analogues under identical conditions. These photoreactions generate VAD, and the independently prepared (Supporting Information) diol **5** and keto-alcohols **6** and **18** (Scheme 4, Table 1). Importantly, keto-alcohol **6** along with VAD is generated when diol **5** is subjected to the DCA-promoted photochemical reaction conditions.

As with the β-O-4 model compounds, DCA-induced photoreactions of **4T** and **4E** yield VAD as the major product, and substrate conversions for fixed time irradiations are enhanced when O_2-saturated solutions of these substrates are irradiated (Table 1). It should be noted that the photoproducts produced in photoreactions of the isomers of **4** and **8** in most cases (VAD, **16**, **17**, **5**, **6**) are known compounds (Supporting Information).

To evaluate the reactivities of cation radicals derived by SET-oxidation, relative quantum yields of the DCA-promoted photoreactions of the isomers of **4** and **8** were determined. Relative quantum efficiencies (ϕ_{rel}) were measured by using the standard simultaneous irradiation technique, in which equivalent concentrations of DCA and substrates are irradiated for equivalent time periods that bring about low substrate conversions (ca. 10%). The data obtained from

SCHEME 4

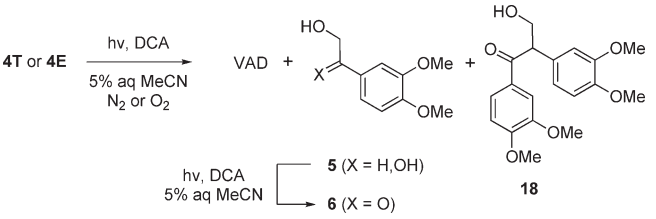

TABLE 2. Relative Quantum Yields of Photoreactions, Oxidation Potentials, and Rates of DCA-Fluorescence Quenching of the Lignin Model Compounds

substrate	ϕ_{rel}[a]	$E^{S}_{1/2}$ (+) (V vs Ag/AgCl)	$k_q \times 10^{-10}$ (M^{-1} s^{-1})
4T	6.5	1.18	1.24
4E	7.7	1.22	1.16
8E	1.9	1.22	1.16
8T	1.0	1.19	0.99

[a]Relative quantum yields for formation of VAD.

SCHEME 5

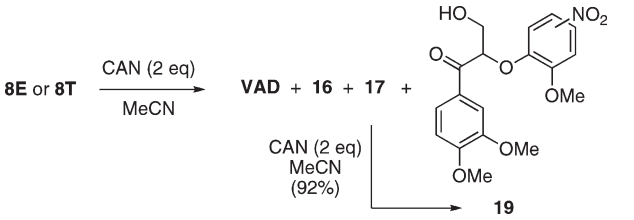

these experiments (Supporting Information) are given in Table 2. To ensure that the relative quantum yields reflect the reactivities of the cation radicals produced by SET to the singlet excited state of DCA (DCA^{S1}) and not the rates of SET to DCA, fluorescence quenching measurements were made. The results displayed in Table 2 show that, in each case, the β-1 and β-O-4 model compounds quench the fluorescence of DCA at near equal diffusion-controlled rates. This is expected based on the fact that the measured oxidation potentials ($E^{S}_{1/2}$ (+)) of the isomers of **4** and **8** (Table 2) all fall well below the reduction potential of DCA^{S1} (+2.8 V).

Ceric Ammonium Nitrate (CAN)-Promoted Reactions of the Lignin Model Compounds. SET-oxidation reactions of **4T**, **4E,** and **8E**, promoted by the one-electron oxidant CAN, also take place predominantly by way of C−C bond cleavage to yield VAD as the major product. For example, reactions of the *erythro* isomer of the β-O-4 model compound with 2 equiv of CAN in MeCN at 25 °C give rise to VAD, keto-alcohol **17**, and a nitro-substituted keto-alcohol **19** of unassigned regiochemistry (Scheme 5, Table 3). The latter substance was shown to arise by secondary CAN oxidation of **17**.

Interestingly, CAN oxidations of the *erythro* and *threo* isomers of **8** give rise to dramatically different ratios of VAD and keto-alcohol **17**. Specifically, while **8E** yields VAD nearly exclusively, near equal amounts of VAD and **17** are produced by reaction of **8T** under equivalent CAN oxidation conditions. This trend is not observed in CAN oxidations of the β-1 models, **4T** and **4E**, where VAD is the predominant product formed along with keto-alcohols **6** and **18** (Scheme 6, Table 3).

CAN-induced oxidation reactions of arenes take place by pathways involving initial SET to Ce (IV) followed by rate limiting reactions of the formed cation radical intermediates (*eg.*, proton transfer, C−C bond cleavage). In contrast, CAN

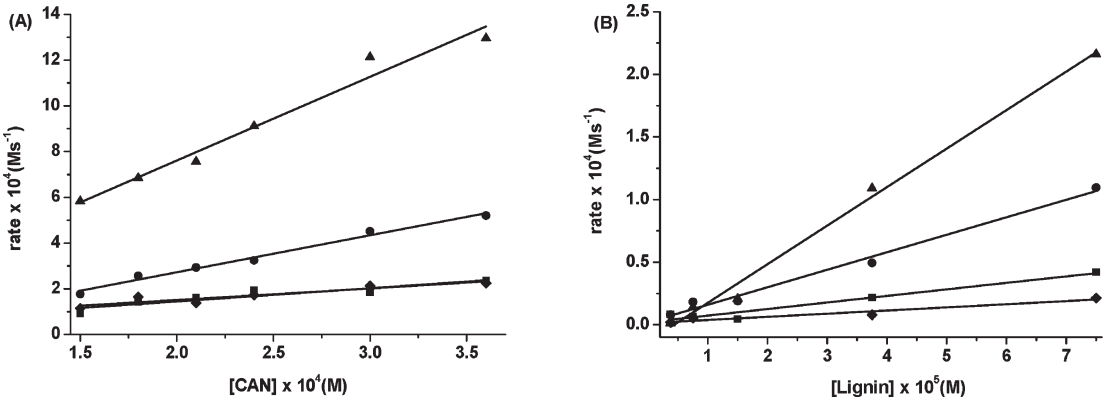

FIGURE 5. Plots of the rates of CAN oxidations of **4T** (▲), **4E** (●), **8E** (■), and **8T** (♦) as (A) functions of the concentration of CAN at fixed concentrations of **4T**, **4E**, **8E**, and **8T** (3.75×10^{-4} M) and (B) functions of the concentrations of **4T**, **4E**, **8E**, and **8T** at fixed concentrations of CAN (3.0×10^{-4} M). The reactions were carried out by using MeCN solutions of the reactants at 25 °C for time periods of 0.1−0.25 s.

TABLE 3. Products and Yields of CAN-Promoted Reactions of the Lignin Model Compounds

		Percent Yields[b]					
substrate	% conv[a]	VAD	**6**	**16**	**17**	**18**	**19**
4T	100	95	25			trace	
4E	100	95	46			trace	
8E	90	88		trace	7		4
8T	96	31		trace	32		33

[a]Reaction of CAN (1.0 mM) and lignin model compound (0.5 mM) in MeCN at 25 °C for 15 h. [b]Yields determined by using HPLC analysis.

SCHEME 6

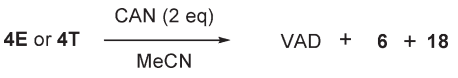

oxidations of arylalkanols occur via SET within a substrate-CAN complex.[59b] As a result, the rates of CAN oxidations of the lignin model compounds could reflect the reactivity of the initially formed cation radicals (see below). If this assumption is correct, the rates of of CAN-promoted VAD production will correspond to rates of cation radical C−C bond cleavage. Indeed, absorbances of CAN (2.5×10^{-4} M initially) at 390 nm in MeCN solutions containing 1.25×10^{-4} M of the lignin model compounds decrease as a function of time. In each case, the absorbance reaches a constant value after 2 equiv of CAN are consumed. A qualitative interpretation of absorbance versus time plots (Figure 5S, Supporting Information) show that the rates of the CAN oxidation reactions are dependent on the nature (β-1 vs β-O-4) and concentrations of the lignin models.

Accurate rate constants for the CAN oxidation reactions of the stereoisomers of **4** and **8** were determined by measuring the initial rates of disappearance of CAN (0.1−0.25 s) by using the stopped flow kinetic technique. Kinetic analyses were carried out under two different conditions including (1) 3.75×10^{-4} M lignin model compounds and varying concentrations (1.5×10^{-4} to 3.6×10^{-4} M) of CAN (Figure 5A) and (2) 3.0×10^{-4} M CAN and varying concentrations (7.5×10^{-5} to 3.75×10^{-6} M) of the lignin models (Figure 5B). The slopes of these plots (at < 10% conversion of substrate) give bimolecular rate constants for the oxidation reactions and, consequently, the rates of reactions of the cation radicals arising from the diastereomers of **4** and **8** (Table 4).

TABLE 4. Rate Constants for CAN Oxidations of the β-O-4 and β-1 Lignin Model Compounds

substrate	$k \times 10^{-2}$ (M^{-1} s^{-1})[a]	$k \times 10^{-2}$ (M^{-1} s^{-1})[b]
4T	98	103
4E	43	47
8E	15	17
8T	14	8

[a]Determined by varying the concentration of CAN at fixed concentrations of the lignin model compounds. [b]Determined by varying the concentration of the lignin model compounds at fixed CAN concentrations.

TABLE 5. Products and Yields of Lignin Peroxidase Catalyzed Reactions of the Lignin Model Compounds[a]

	percent yields[b]				
substrate	VAD	**5**	**6**	**16**	**17**
4T	71	trace	19		
4E	58	trace	19		
8E	86			trace	11
8T	47			trace	44

[a]Reactions carried out using 200 μM substrate, 0.36 μM LP, 100 μM H_2O_2 in tartrate buffered solutions (pH 3.4). [b]Yields based on recovered substrated, determined by using HPLC.

Lignin Peroxidase Catalyzed Reactions of the lignin Model Compounds. The LP-catalyzed C−C bond cleavage reactions of the β-1 and β-O-4 models were carried out in the presence of H_2O_2, which promotes a 2-electron oxidation to form LP-I that in turn oxidizes two molecules of substrate (Figure 2).[31−37] The products and yields of the LP-catalyzed reactions of the β-1 and β-O-4 models with 0.5 equiv of H_2O_2 were determined by using HPLC analysis (Table 5). The reactions of β-1 *erythro* and *threo* isomers **4T** and **4E** generated VAD, diol **5**, and keto-alcohol **6** as the major products in near quantitative yields based on recovered substrate. The reactions of β-O-4 *erythro* and *threo* isomers **8E** and **8T** cleanly generate VAD and keto-alcohol **17** as the major products and guaiacol **16** as a minor product.

Kinetic studies of the LP-catalyzed reactions of the β-1 and β-O-4 models were carried out. Initial reaction rates were determined from the time courses for product formation (VAD plus keto-alcohol were continuously monitored at 310 nm). Since H_2O_2 also inactivates LP, times courses as a function of enzyme, substrate, and H_2O_2 concentrations (data not shown) were determined in order to identify the optimal conditions for analysis of the reaction rates of the

TABLE 6. Steady State Kinetic Constants for Lignin Peroxidase Catalyzed Reactions of the β-O-4 and β-1 Lignin Model Compounds[a]

substrate	k_{cat} (s^{-1})	K_M (μM)	$k_{cat}/K_M \times 10^4$ (μM^{-1} s^{-1})
4T	3.9	50	8
4E	9.2	250	4
8E	0.50	160	0.3
8T	1.14	130	1

[a]Reaction solutions initially contained 1.8 μM LP, 50 μM H_2O_2, and 0.05−2.5 mM substrate in 125 mM tartrate (pH 3.5; 25 °C).

β-1 and β-O-4 models. The results show that the loss of LP activity can be minimized by limiting the assay time and by employing a substrate:H_2O_2 ratio equal to or greater than unity. These conditions were best accommodated by using the LP at a high concentration (1.8 μM) to ensure rapid product formation and employing a stopped flow UV system to mix LP with the buffered substrate plus H_2O_2 and to monitor product formation over a 1 s reaction period. To determine the steady-state kinetic constants (k_{cat} and K_m), the initial reaction rates were measured over a substrate concentration range of 0.05 to 2.5 mM and at a fixed H_2O_2 concentration of 50 μM. All plots of A_{310} versus time, used to define initial rates (by slope calculation), were linear. The steady-state kinetic constants, reported in Table 6, were calculated from the initial rate versus substrate concentration data (plotted in Figures S2 and S3 in Supporting Information).

Discussion

The overall aim of our studies in this area is to gain fundamental information about the factors that govern the oxidative carbon−carbon bond cleavage reactivity of various 1,2-diaryl- and 1-aryl-2-aryloxy-propanoid units found in the structurally and stereochemically complex natural polymer lignin. We believe that knowledge obtained in an effort of this type will aid in the design of methods that can be used to degrade lignin in a mild, efficient, and cost-effective manner as part of processes that transform plant materials into ethanol. As described in the Introduction, one of the most promising approaches to promote plant delignification involves the use of enzymes derived from wood rotting fungi, such as *Phanerochaete chrysosporium*.[19−22] The most studied of these enzymes is lignin peroxidase (LP), which is believed to promote delignification by oxidative C1−C2 bond cleavage of aryl propanoid moieties in lignin by way of a mechanism that is initiated by single electron transfer (SET) from aryl donor sites to the $Heme^{+1}$-Fe^{4+} form of the enzyme. Key events in the degradation pathway are C−C bond cleavage reactions of aryl ring centered lignin cation radicals. These

SCHEME 7

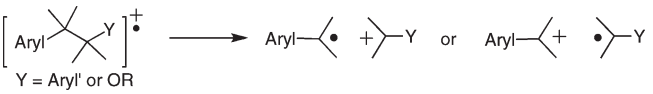

processes, which mimic reactions of the cation radicals of 1,2-diarylethanes and 1-aryl-2-ethyl ethers (Scheme 7),[59−72] result in the generation of cation radical pairs in which odd electron and positive charge distributions are governed by thermodynamics. As has been pointed out previously and experimentally demonstrated in thorough studies by Arnold and his co-workers,[61−66] the C−C bond cleavage reactions of cation radicals of these types of substrates can be viewed as being either heterolytic or homolytic in nature, and in either case they yield the most stable radical and cation intermediates. Perhaps more significant are observations made by Arnold[61−66] and Maslak[67−71] which show that the rates of C−C bond cleavage of 1,2-diarylethane and 1-aryl-2-ethyl ether cation radicals parallel cation radical C−C bond dissociation energies. This important concept will be fully discussed below following a discussion of reaction mechanisms and observations leading to the assignments of C−C bond cleavage rates of the diastereomeric β-1 and β-O-4 lignin model compounds.

Reaction Mechanisms. In the current investigation, three methods were used to generate cation radicals of the diastereomeric β-1 and β-O-4 lignin model compounds. The first of these involves the use of a SET-photochemical route in which the UV irradiation generated singlet excited state of DCA (DCA^{S1}) ($E_{1/2}$ (−) = +2.8 V, vs SCE) serves as the oxidant. As demonstrated by the results of DCA fluorescence quenching experiments, the lignin model compounds quench DCA^{S1} at near equal, diffusion-controlled rates (ca. 1×10^{10} M^{-1} s^{-1}). Owing to the low oxidation potentials of the model compounds ($E_{1/2}$ (+) ca. 1.2 V vs Ag/AgCl, Table 2) and the fact that the energies of their singlet excited states are much higher than that of DCA, the quenching process takes place by thermodynamically driven (ΔG^0_{SET} = ca. −1.6 eV) SET.[73]

As in the case of reactions initiated by other oxidants, the cation radicals, produced by photoinduced SET of the β-1 and β-O-4 model compounds, undergo predominant C1−C2 bond cleavage to form radical cation pairs. Based on a qualitative evaluation of oxidation potentials,[74] cation radicals arising from the β-1 models **4T** and **4E** have charged radical centers that are nearly equally distributed in both the 1- and 2-aryl rings (Scheme 8). A consideration of approximate oxidation potentials of the two radicals that could be produced suggests that C−C bond cleavage of these transients will produce pairs in which the positive charge is located on the α-hydroxylbenzyl fragment **20** and the radical center is located on the α-hydroxyethylbenzyl fragment **21** (Scheme 8). Data that support this proposal come from the work of

(59) (a) Trahanovsky, W. S.; Brixius, D. W. *J. Am. Chem. Soc.* **1973**, *95*, 6778. (b) Nave, P. M.; Trahanovsky, W. S. *J. Am. Chem. Soc.* **1970**, *92*, 1120.
(60) Davis, H. F.; Das, P. K.; Reichel, L. W.; Griffin, G. W. *J. Am. Chem. Soc.* **1984**, *106*, 6968.
(61) Arnold, D. R.; Maroulis, A. J. *J. Am. Chem. Soc.* **1976**, *98*, 5931.
(62) Arnold, D. R.; LaMont, L. J. *Can. J. Chem.* **1989**, *67*, 2119.
(63) Okamoto, A.; Snow, M. S.; Arnold, D. R. *Tetrahedron* **1986**, *42*, 6175.
(64) Okamoto, A.; Arnold, D. R. *Can. J. Chem.* **1985**, *63*, 2340.
(65) Popielarz, R.; Arnold, D. R. *J. Am. Chem. Soc.* **1990**, *112*, 3068.
(66) Perrott, A. L.; Arnold, D. R. *Can. J. Chem.* **1992**, *70*, 272.
(67) Maslak, P.; Asel, S. L. *J. Am. Chem. Soc.* **1988**, *110*, 8260.
(68) Maslak, P.; Chapman, W. H., Jr. *J. Chem. Soc., Chem. Commun.* **1989**, *23*, 1809.
(69) Maslak, P.; Chapman, W. H., Jr. *Tetrahedron* **1990**, *46*, 2715.
(70) Maslak, P.; Chapman, W. H., Jr.; Vallombroso, T. M., Jr.; Watson, B. A. *J. Am. Chem. Soc.* **1995**, *117*, 12380.
(71) Maslak, P.; Chapman, W. H., Jr. *J. Org. Chem.* **1996**, *61*, 2647.
(72) For studies of related cation radical C−C bond fragmentation processes, see: Baciocchi, E.; Bietti, M.; Lanzalunga, O. *Acc. Chem. Res.* **2000**, *33*, 243. Gaillard, E. R.; Whitten, D. G. *Acc. Chem. Res.* **1996**, *29*, 292. Dinnocenzo, J. P.; Simpson, T. R.; Zuilhof, H.; Todd, W. P.; Heinrich, T. *J. Am. Chem. Soc.* **1997**, *119*, 987. Zu, Z.; Falvey, D. E.; Yoon, U. C.; Mariano, P. S. *J. Am. Chem. Soc.* **1997**, *119*, 145.
(73) Rehm, D.; Weller, A. *Isr. J. Chem.* **1970**, *8*, 259.
(74) This estimate is based on the fact that both aryl rings in the β-1 models are 1-alkyl-3,4-dimethoxy substituted.

SCHEME 8

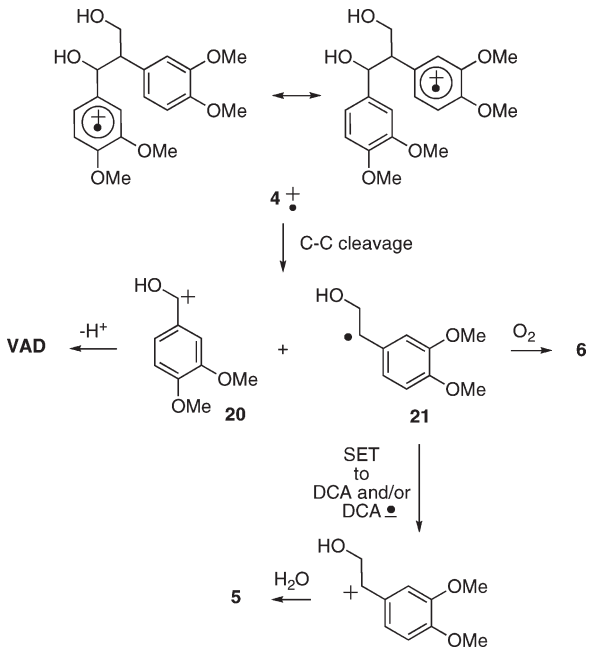

Griller and Wayner,[75−77] which shows that oxidation potentials of oxy-substituted radicals are much lower than those of alkyl-substituted counterparts. For example, the α-methoxy-*p*-methoxybenzyl radical has an oxidation potential of −0.51 V (vs SCE), whereas the α,α-dimethylbenzyl radical has an oxidation potential of −0.14 V (vs SCE).[76,77]

Loss of a proton from **20** gives rise to veratrylaldehyde (VAD), the major product formed in these reactions. The behavior of the radical fragment **21** is different than that observed for related benzylic radicals produced in 1,4-dicyanobenzene (DCB)-photosensitized reactions of 1,2-diphenylethane derivatives. In earlier studies, Arnold and his co-workers[63−65] observed that DCB-promoted cleavage of 1,1,2,2-tetraphenylethane in 3:1 MeCN/MeOH leads to production of diphenylmethylether and diphenylmethane. The formation of the latter substance involves reduction of the intermediate diphenylmethyl radical by the anion radical of DCB. Protonation of the resulting anion then forms diphenylmethane (Scheme 9).

Importantly, no products arising via reduction of radical **21** (Scheme 8) by DCA$^{\bullet}$ are formed in the DCA photoinduced reactions of **4T** and **4E**. Instead, **21** is transformed to the diol **5** and α-hydroxyketone **6**. The former substance arises by oxidation of **21** through SET to DCA or H-DCA$^{\bullet}$ followed by water addition to the resulting cation. In contrast, α-hydroxyketone **6** might arise by addition of adventitious dioxygen to **21** or addition of superoxide (O_2^{S1}), produced by reaction of dioxygen with DCA^{S1}. The observation that **6** becomes a major product when photoreactions of **4T** and **4E** are carried out in dioxygen-saturated solutions supports these proposals for its origin.

UV-spectroscopic monitoring of the reactions of **4T** and **4E** in N_2-saturated solutions shows that DCA is consumed.

SCHEME 9

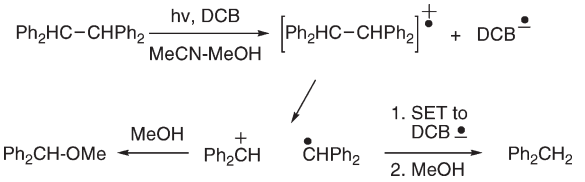

However, this is not the case for the corresponding reactions in O_2-saturated solutions (see Figure S4 in Supporting Information). The disappearance of DCA under the N_2-saturated conditions is responsible for the low conversions seen in the photoreactions and is consistent with the proposal that diol **5** forms by SET from **21** to DCA or HDCA$^{\bullet}$. The effect of O_2 in facilitating DCA-promoted photoreactions of the lignin model compounds (see Table 1) is attributable to its ability to oxidize DCA anion radical or HDCA$^{\bullet}$, which results in regeneration of DCA. However, in light of a number of early studies, which were directed at probing singlet oxygen (O_2^{S1})-promoted oxidative cleavage reactions of lignin[78−81] and lignin model compounds,[57i] it is necessary to consider an alternative manner by which O_2 participates in these photoreactions. Although mechanistically difficult to rationalize, it is possible that when oxygen is present in reasonably high (ca. 3 mM in O_2-saturated solutions) concentrations, the conversion of the *β*-1 lignin model compounds to VAD, diol **5**, and ketoalcohol **6** might be promoted by O_2^{S1}. However, on the basis of the results of more recent investigations,[82−84] perhaps most notably the one carried out by Eriksen and Foote,[83] along with a consideration of (1) substrate versus oxygen concentrations, (2) rates of SET from the models versus energy transfer from O_2 to DCA^{S1}, and (3) chemical reasoning, it seems highly unlikely that O_2^{S1} is formed to an appreciable extent in these reactions and that even if it were it would promote C−C bond cleavage processes.

The comparison of DCA-promoted photoreactions of the *β*-1 model compounds and DCB-photosensitized reactions of 1,1,2,2-tetraphenylethane and its derivatives is interesting. As pointed out above, in the DCB-promoted reactions studied earlier by Arnold and his co-workers, diphenylmethyl radicals formed by C−C bond cleavage reactions participate as electron acceptors in SET with the DCB anion radical (Scheme 9). In contrast, the dimethoxy-substituted benzyl radical **21**, paired with the DCA anion radical, is instead oxidized to produce the cation precursor of diol **5**. Several factors might be responsible for this difference. First, as a more stable anion radical is less prone to donate an electron to benzylic radicals. This property is reflected in the larger reduction potential of DCA (ca. −0.9 V, vs SCE)[85] versus DCB (ca. −1.7 V, vs SCE),[63] which indicates the

(75) Wayner, D. D. M.; McPhee, D. J.; Griller, D. *J. Am. Chem. Soc.* **1988**, *110*, 132.
(76) Sim, B. A.; Milne, P. H.; Griller, D.; Wayner, D. D. M. *J. Am. Chem. Soc.* **1990**, *112*, 6635.
(77) Wayner, D. D. M.; Sim., B. A.; Dannenberg, J. J. *J. Org. Chem.* **1991**, *56*, 4853.
(78) Bonini, C.; D'Auria, M. D.; D'Alessio, L. D.; Mauriello, G.; Tofani, D.; Viggiano, D.; Zimbardi, F. *J. Photochem. Photobiol. A* **1998**, *113*, 119.
(79) Bonini, C.; D'Auria, M. D.; D'Alessio, L. D.; Mauriello, G.; Tofani, D.; Viggiano, D.; Zimbardi, F. *J. Photochem. Photobiol. A* **1998**, *118*, 107.
(80) Bentivenga, G.; Bonini, C.; D'Auria, M.; De Bona, A.; Mauriello, G. *Chemosphere* **1999**, *14*, 2409.
(81) Bentivenga, G.; Bonini, C.; D'Auria, M.; De Bona, A. *J. Photochem. Photobiol. A* **1999**, *128*, 139.
(82) McNally, A. M.; Moody, E. C.; McNeill, K. *Photochem. Photobiol. Sci.* **2005**, *4*, 268.
(83) Eriksen, J.; Foote, C. S. *J. Am. Chem. Soc.* **1980**, *102*, 6083.
(84) Kojima, M.; Kuriyama, Y.; Sakuragi, H.; Tokumaru, K. *Bull. Chem. Soc. Jpn.* **1991**, *64*, 2724.
(85) Chandross, E. A.; Ferguson, J. *J. Chem. Phys.* **1967**, *47*, 2557.

relative stability and reducing ability of the corresponding radical anion. Second, although the reduction potential of the α-alkyl-dimethoxyphenyl substituted benzyl radical **21** is not known, it is predicted to be low and, thus, that the radical would be difficult to reduce. This is seen in the comparison of the known reduction potentials of the diphenylmethyl radical ($Ph_2HC^{\bullet}$ −1.14 V, vs SCE)[75] versus that of the *p*-methoxycumyl radical (*p*-$MeOC_6H_4C^{\bullet}Me_2$, −1.9 V, vs SCE)[76] which models **21**. Finally, the very low oxidation potentials of ring-methoxy and α-alkyl-substituted benzyl radicals (e.g., −0.14, vs SCE for *p*-$MeOC_6H_4C^{\bullet}Me_2$)[77] suggest that **21** will have a much greater propensity to be oxidized than reduced.

A comment about the origin of β-hydroxyketone **18**, formed in DCA-promoted photoreactions of **4T** (8%) and **4E** (trace), is in order. This substance most likely arises by loss of the C-1 benzyl proton in the initially formed cation radical intermediates. This common reaction pathway[86] leads to formation of a benzylic radical, which following SET-oxidation and loss of a proton yields **18**.

Mechanistic pathways similar to those discussed above are involved in DCA-promoted photoreactions of the β-O-4 model compounds **8E** and **8T**. In the β-O-4 radical cations, the charged radical center should be more highly localized on the C-1 aryl rather than 2-aryloxy ring (Scheme 10).[87] Carbon−carbon bond cleavage in these radical cations produces a radical cation pair in which the positive charge resides on the hydroxybenzylic component **20** and the radical on the aryloxyalkyl part **22**. As in the pathway for reactions of the β-1 models, deprotonation of **20** forms VAD and an oxidation-hydrolysis sequence transforms **22** to guaiacol. Finally, the cation radicals derived from **8E** and **8T** also undergo benzylic deprotonation to yield precursors of the β-hydroxyketone **17**. Although this is only a minor pathway followed in reactions of the β-1 models and the β-O-4 *erythro* isomer, loss of the C-1 benzylic proton from the cation radical of **8T** is highly competitive with C−C bond cleavage.

Product Distributions. Despite the fact that different SET oxidants are involved and widely different conditions are employed, the DCA-, CAN-, and LP-promoted reactions of the lignin model compounds produce remarkably similar product distributions. In almost all of these processes, C1−C2 bond cleavage products (e.g., VAD) predominate. To varying extents and depending on the nature of the model (β-1 vs β-O-4) and stereochemistry (*erythro* vs *threo*), β-hydroxyketone products arising by benzylic oxidations are also generated. Interesting in this regard are the DCA-, CAN-, and LP-promoted reactions of the diastereomeric β-O-4 models where benzylic oxidation is the minor (for **8E**) or major (for **8T**) route followed. For example, β-hydroxyketone **17** is formed in low yields (5−11%) in all types of oxidation reactions of **8E**. In comparison, this ketone and its nitro-derivative **19** are generated in yields ranging from 22% to 65% in oxidation reactions of **8T**. This difference is dramatized in the CAN reactions of **8E** and **8T**, where C−C bond cleavage (i.e., formation of VAD) dominates by 12:1 over benzylic oxidation in **8E** and becomes a minor process (1:2) in CAN oxidation of **8T**.

SCHEME 10

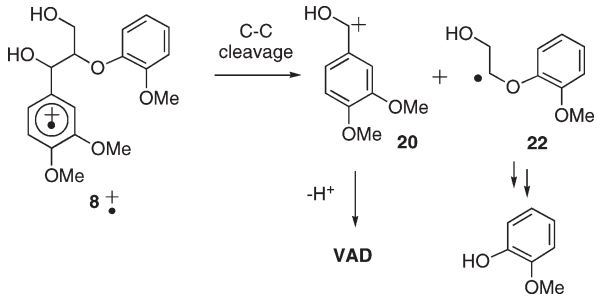

The difference observed in the nature of the dominant pathways followed in reactions of cation radicals arising from **8E** and **8T** (and to a lesser extent with **4E** and **4T**) are likely a consequence of stereoelectronic effects. As Arnold demonstrated earlier in investigations with phenylcyclopentane derivatives,[66] C1−C2 bond cleavage in cation radicals of 1-phenylethanes requires the availability of conformations in which the vulnerable C−C bond overlaps with the SOMO of the arene localized cation radical. When this requirement is not met and benzylic C−H SOMO overlap is preferred, deprotonation of the cation radical takes place. Thus, the source of the differences in the C−C vs C−H bond cleavage reactivity of the **8E** and **8T** cation radicals (and to a lesser extent with **4E** and **4T**) might be associated with differences in C1−C2 bond conformational preferences in cation radicals of the two diastereomers.

Additional observations made in reviewing the product distributions deserve brief comment. As mentioned above, the major products generated in the DCA-, CAN-, and LP-promoted reactions of the β-1 model compounds are VAD, diol **5**, and ketoalcohol **6**. The latter two products arise from the C2−C3 fragment of each of the models. In contrast, oxidations of the β-O-4 models yield only small amounts of guaiacol, which also corresponds to a portion of the C2−C3 fragment. This finding, which matches those made by others in studies of enzymatic and nonenzymatic reactions of β-O-4 models (see above), is likely caused by the instability of guaiacol under oxidative conditions. Finally, the formation of nitroaryl ketone **19** in CAN oxidations of **8E** and **8T** is interesting. This substance arises by secondary oxidation of the initially formed ketone **17**. While arene nitration reactions of this type are well-documented,[88] why the process occurs only in the case of the β-O-4 models and only on the aryloxy ring of the ketone and not the starting substrate is difficult to understand.

Cation Radical C−C Bond Cleavage Rates. One of the main aims of this study was to determine how both structural (β-1 vs β-O-4) and stereochemical (*erythro* vs *threo*) features govern the C−C bond cleavage reactivities of cation radicals arising by SET-oxidation of lignin model compounds. As described above, three different methods were employed to generate the cation radicals of the models, and three different techniques were used to obtain C−C bond cleavage rate data. These include measurements of relative quantum yields of DCA-promoted photoreactions and the rates of CAN- and LP-induced oxidations. For the data coming from studies of the DCA-promoted and CAN- and LP-induced

(86) Sheldon, R. A.; Kochi., J. K. *Metal Catalyzed Oxidations of Organic Compounds*; Academic Press: NY, 1981.

(87) This prediction is based on the fact that the C1-aryl ring is 1-alkyl-3,4-dialkoxy substituted whereas the C2-aryl ring is 1,2-dialkoxy substituted.

(88) Grenier, J.-L.; Catteau, J.-P.; Cotelle, P. *Synth. Commun.* **1999**, *29*, 1201.

TABLE 7. Relative Rates of C−C Bond Cleavage in Cation Radicals Arising from SET-Oxidation of Lignin Model Compounds

	relative rates		
model	from DCA-promoted reactions	from CAN-promoted reactions	from LP-promoted reactions
4T	5	25	53
4E	7	11	123
8E	2	4	1
8T	1	1	1

reactions to have meaning, account needs to be taken of how the measurement were made and, consequently, their relationship to cation radical C−C bond cleavage rates.

The relative quantum yields for VAD formation (Table 2) in the DCA-promoted photoreactions, determined under identical conditions and at low conversions should be directly proportional to the related rates of C−C bond cleavage. Specifically, when equivalent concentrations of DCA and each lignin model are used in simultaneous irradiation experiments, equivalent numbers of photons are absorbed by DCA and an equivalent fraction of DCA^{S1} is being quenched by SET from the lignin models when corrections are made using the k_q values given in Table 2. Cation radicals produced in the SET step can undergo C−C bond cleavage to form VAD along with highly exothermic back electron transfer (BSET) to $DCA^{\bullet}$. Consequently, differences in the quantum yields for VAD formation are directly related to differences in the rate constants for cation radical C−C bond cleavage. The relative C−C bond cleavage rates, obtained from an analysis of the relative quantum yield data and correcting for differences in the rates for DCA^{S_1} quenching, are given in Table 7.

The rate constants determined for CAN-promoted oxidations of the lignin models are based on the rates of CAN disappearance. Consequently, they only partially reflect the rates of cation radical C−C bond cleavage owing to the fact that the observed rates are also a function of the rates of initial complex formation,[59b] intracomplex SET from the models to Ce(IV), and BSET as well as other oxidation reactions (e.g., benzylic oxidation). If the assumption that both SET and BSET rates will be the same for each model compound, the observed rates given in Table 4 are directly proportional to C−C bond cleavage rates if account is taken for the proportion of competitive benzylic oxidation taking place. This is especially true in the case of the β-O-4 models **8E** and **8T** where a significant fraction of the process involves benzyl C−H rather than C1−C2 bond cleavage. Since the CAN oxidation kinetic measurements were made at very short reaction times and correspondingly low conversion, correction for the formation of **17** and **19**, both arising by benzylic oxidation, does not have to be performed separately. Thus, after correcting for competitive formation of **17** + **19** from **8E** and **8T**, the averages of the rate data in Table 4 become the relative cation radical C−C bond cleavage rates listed in Table 7.

Finally, owing to the method used for kinetic analysis, k_{cat} values for LP-catalyzed reactions of the lignin models correspond to the formation of all products that absorb at 310 nm. Thus, in order to determine the rates of C−C bond cleavage that yields VAD, the extinction coefficients at 310 nm of VAD (1.06×10^4) and ketoalcohols **6** (0.95×10^4) and **17** (1.06×10^4) along with the relative amounts of each substance produced in the LP-promoted processes must be considered. Treatment of the k_{cat} values in Table 6 in this manner yields the relative rates of cation radical C−C bond cleavage derived from analysis of the kinetics of enzymatic reaction given in Table 7.

The relative rate data arising from kinetic analyses presented above contain several interesting features and possible anomalies related to the cation radical C−C bond cleavage process. First, although stereochemistry of the β-1 and β-O-4 compounds definitely influences bond cleavage rates, the trends vary depending on the oxidation conditions employed. For example, the cation radical of the *erythro* diastereomer of the β-1 model **4E** is transformed more rapidly to VAD under the conditions used in the DCA photochemical and LP-catalyzed reactions. In contrast, the *threo* isomer **4T** is more reactive than **4E** in CAN-promoted reactions. Likewise, the β-O-4 *erythro* isomer **8E** undergoes C−C bond cleavage more rapidly than the *threo* analogue **8T** under both DCA and CAN conditions, and **8E** and **8T** are about equally reactive in the LP-catalyzed process. It is possible that the stereochemistry versus rate differences in the CAN-promoted reactions could be a consequence of the fact that only in this case does SET occur within a complex formed between the substrate and oxidant.[59b]

It should be noted that the results of earlier studies[89−91] of metal oxidation and LP reactions, although mixed,[92] showed that the rates of disappearance of **8T** exceeds that of **8E**. However, to our knowledge in no previous effort have the relative rate data been adjusted to account for the fact that **8T** reacts by competitive C−C and C−H bond cleavage pathways to produce VAD and ketoalcohol **17**, respectively. When this fact is taken into account, the rates of C−C bond cleavage of the **8E** cation radical becomes larger than or near equal to that of the **8T** cation radical.

The most significant observation made in the current investigation is that, independent of the method used and stereochemistry, cation radicals derived from the β-1 lignin models undergo C−C bond cleavage at rates that far exceed those of the β-O-4 models. The β-1:β-O-4 rate ratios range from 7:1 to 123:1 when the most reactive versus least reactive stereoisomer in each series is compared. This finding has both mechanistic and potentially practical significance.

Analysis of Rates. As has been discussed earlier in the pioneering work of Arnold and later by Maslak and others, the reactivity of radical cations generated by SET-oxidation of substituted 1,2-diarylethanes and 1-aryl-2-ethyl ethers appears to be governed by cation radical C−C bond dissociation energies (BDEs) and conformations. With some simple aryl-substituted ethanes, it is possible to calculate or estimate radical cation BDEs by using simple thermochemical cycles.[62] In these cycles, the energy required to produce the radical cation pair is composed on one hand of the BDE of the neutral substrate and the oxidation potential of the more easily oxidized radical product and, on the other hand, of the oxidation potential of the substrate and the BDE of the cation radical. Consequently, knowing the substrate oxidation potential and C−C BDE and $E_{1/2}$ (+) of the most easily

(89) Bohlin, C.; Anderson, P.-O.; Lundquist, K.; Jönsson, L. J. *J. Mol. Catal. B* **2007**, *45*, 21.
(90) Bohlin, C.; Lundquist, K.; Jönsson, L. J. *Enzyme Microb. Technol.* **2008**, *43*, 199.
(91) Bohlin, C.; Lundquist, K.; Jönsson, L. J. *Bioorg. Chem.* **2009**, *37*, 143.
(92) Rochefort, D.; Bourbonnais, R.; Leech, D.; Paice, M. G. *Chem. Commun.* **2002**, 1182.

oxidized radical, it is possible to calculate the cation radical BDE. Unfortunately, despite the detailed studies by Griller and Wayner,[75−77] only a small number of radical oxidation potentials are known. In addition, C−C BDEs of highly substituted diarylethanes and arylethyl ethers have not been determined. Thus, insufficient information is available to determine the cation radical BDEs of the β-1 and β-O-4 models.

Inspection of reactivity profiles of substances that might be considered as simple models of the β-1 (diarylethanes) and β-O-4 (arylethyl ethers) models deceivingly suggests that cation radicals of the latter substances should undergo more rapid C−C bond cleavage. Accordingly, Arnold[63] showed that in contrast to 1,1,2-triphenylethane, whose SET-generated cation radical is unreactive, the 1,1-diphenyl-2-ethyl ether cation radical undergoes smooth C−C bond cleavage. On the basis of this observation, one might predict that cation radicals arising from the β-O-4 substrates (complex arylethyl ethers) would undergo C−C bond cleavage more readily than those of the β-1 models (complex diarylethanes). However, the results of qualitative evaluations of roughly estimated thermochemical cycles suggest that the C−C BDEs of β-1 cation radicals should be lower than those of their β-O-4 counterparts. Specifically, since the oxidation potentials of the β-1 and β-O-4 model compounds are roughly equal and the same radical is oxidized to form the cationic intermediate **20** in both thermochemical cycles, the relative cation radical BDEs of the β-1 and β-O-4 compounds should be directly related to the BDEs of the neutral substrates. Although the values are not known, the BDEs of the simple analogues, 1,2-diphenylethane (64 kcal/mol)[93] and 1-phenylethyl phenyl ether (77 kcal/mol),[94] have been calculated. This comparison suggests that the cation radical BDEs of the β-1 compounds should be lower than those of the β-O-4 analogues. Clearly, contributions made by methoxy substituents on the arene rings and the hydroxyl and hydroxymethyl groups found in **4** and **8** need to be considered in this analysis since they should have profound impacts on cation radical C−C bond dissociation energies.

Theoretical Considerations. To gain a more accurate assessment of the C1−C2 bond cleavage reactivity of cation radicals of the lignin model compounds, density functional theory (DFT) calculations were performed. Geometry optimizations were carried out using DFT with a B3LYP hybrid exchange correlation function and the 6-31+G(d,p) basis set in the gas phase using the Gaussian 09 program.[95] In each case, lowest energy conformations (among many local minima) of the neutral lignin models **4T**, **4E**, **8T** and **8E** and their corresponding cation radicals were obtained by means of frequency calculations (see Supporting Information for energies and atomic coordinates). The minimum energy conformations were employed in determining the BDEs, bond angles, and orbital coefficients presented and discussed below. BDEs of the neutral lignin model compounds were calculated by using differences in energies between the neutral compounds and those of the corresponding radicals obtained by homolytic C1−C2 bond cleavage. Cation radical BDEs were calculated by using differences in energies between the optimized model cation radicals and the two sets of radical cation pairs that are generated by cation radical C1−C2 bond fragmentation. All radical and cation fragments used in the BDE calculations were fully optimized. In addition, MP2/6-31+G(d,p) calculations using the DFT optimized geometries were performed in order to determine the ionization potentials (IP) of the neutral model compounds.

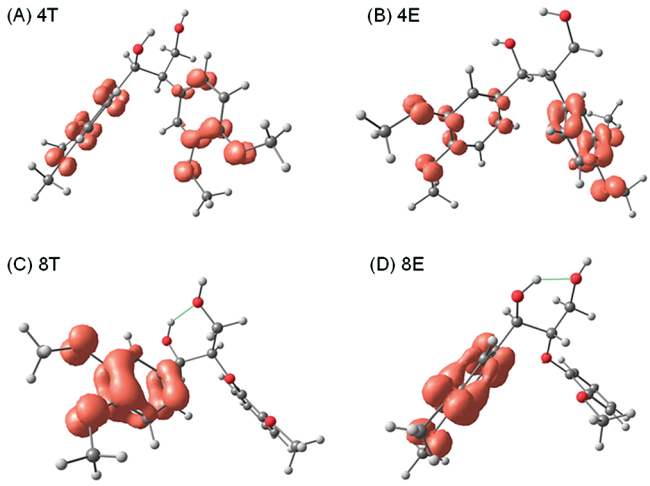

FIGURE 6. DFT energy minimized structures and orbital coefficients representing the odd electron (positive charge) densities in cation radicals derived from the lignin model compounds **4T**, **4E**, **8T**, and **8E**. Isosurfaces correspond to 0.004 au in all of the compounds.

The energy minimized structures of the cation radicals of **4T**, **4E**, **8T**, and **8E** are given in Figure 6. The DFT calculations suggest that the cation radical of **4T** is 3.6 kcal/mol lower in energy than that of **4E** and **8E** is 2.5 kcal/mol more stable than **8T**.

Energy minimized structures of the cation radicals containing pictorial representations of orbital coefficients that reflect odd electron (and positive charge) densities are given in Figure 6. As expected (see above), owing to the large oxidation potential difference between the C1- and C2-arene rings in the β-O-4 compounds **8T** and **8E**, odd electron and positive charge densities in the corresponding cation radicals reside heavily on the C1-arene moiety. In contrast, each β-1 model contains arene rings that should have near equal oxidation potentials (i.e., both are monoalkyl, dimethoxy substituted). This prediction is consistent with the calculation results, which show that odd electron densities are nearly the same in both arene rings of the cation radicals of these substances.

More pertinent to the issue of cation radical reactivities are the calculated C1−C2 BDEs of the neutral and cation radical states of the lignin model compounds (Table 8). In addition, two C1−C2 BDEs are given for each cation radical since

(93) Camaioni, D. M. *J. Am. Chem. Soc.* **1990**, *112*, 9475.
(94) Beste, A.; Buchanan, A. C., III *J. Org. Chem.* **2009**, *74*, 2837.
(95) Frisch, M. J.; Trucks, G. W.; Schlegel, H. B.; Scuseria, G. E.; Robb, M. A.; Cheeseman, J. R.; Scalmani, G.; Barone, V.; Mennucci, B.; Petersson, G. A.; Nakatsuji, H.; Caricato, M.; Li, X.; Hratchian, H. P.; Izmaylov, A. F.; Bloino, J.; Zheng, G.; Sonnenberg, J. L.; Hada, M.; Ehara, M.; Toyota, K.; Fukuda, R.; Hasegawa, J.; Ishida, M.; Nakajima, T.; Honda, Y.; Kitao, O.; Nakai, H.; Vreven, T.; Montgomery, Jr., J. A.; Peralta, J. E.; Ogliaro, F.; Bearpark, M.; Heyd, J. J.; Brothers, E.; Kudin, K. N.; Staroverov, V. N.; Kobayashi, R.; Normand, J.; Raghavachari, K.; Rendell, A.; Burant, J. C.; Iyengar, S. S.; Tomasi, J.; Cossi, M.; Rega, N.; Millam, N. J.; Klene, M.; Knox, J. E.; Cross, J. B.; Bakken, V.; Adamo, C.; Jaramillo, J.; Gomperts, R.; Stratmann, R. E.; Yazyev, O.; Austin, A. J.; Cammi, R.; Pomelli, C.; Ochterski, J. W.; Martin, R. L.; Morokuma, K.; Zakrzewski, V. G.; Voth, G. A.; Salvador, P.; Dannenberg, J. J.; Dapprich, S.; Daniels, A. D.; Farkas, Ö.; Foresman, J. B.; Ortiz, J. V.; Cioslowski, J.; Fox, D. J. *Gaussian 09*; Gaussian, Inc.: Wallingford CT, 2009.

TABLE 8. DFT Calculated C1−C2 Bond Dissociation Energies of 4T, 4E, 8T, and 8E and Their Corresponding Cation Radicals

			BDEs of cation radicals forming	
models	ionization potentials (eV)	BDE of neutral models (kcal/mol)	C1-benzylic cations (kcal/mol)	C2-benzylic/ aryloxy cations (kcal/mol)
4T	7.63	54.0	30.5	36.2
4E	7.87	55.8	24.8	35.2
8T	7.64	75.3	37.2	46.4
8E	7.55	63.9	38.1	45.8

homolytic and heterolytic fragmentations of these species can give two sets of cation radical pairs. As anticipated (see above), the calculations show that a large energetic preference exists for C1−C2 bond cleavage reactions of the cation radicals of **4T**, **4E**, **8T**, and **8E** that generate the 3,4-dimethoxy-α-hydroxymethyl benzylic cation (see **20** in Scheme 8) rather than the corresponding C2-benzylic (from **4T** and **4E**) or aryloxy (from **8T** and **8E**) cations.

The results of the BDE calculations for the neutral lignin models are in good agreement with previously reported values, calculated for the less methoxy and alkyl substituted analogues, 1,2-diphenylethane[93] and 1-phenylethyl phenyl ether.[94] Moreover, the large reduction in the C1−C2 BDEs seen upon going from the neutral to the cation radical states of the models matches the theoretical results reported by Camaioni[93] and the earlier reports by Arnold.[61,62] Significantly, the relative BDEs, which should reflect rates of C1−C2 bond cleavage, are in complete accord with the experimentally determined relative reactivities of the β-1 and β-O-4 cation radicals of the lignin model compounds. Accordingly, the large (ca. 7−14 kcal/mol) differences that exist between the BDEs of **4T** and **4E** versus **8T** and **8E** correlate with the greater reactivities of cation radicals derived by one-electron oxidation reactions of the β-1 models, promoted by using the DCA-photosensitization, CAN, and LP conditions. It should be noted that the gas phase calculations on charged/radical species are useful in estimating energy differences between species with similar charge characteristics. The preliminary results from ongoing studies, which utilize calculations that take into account the effects of a high dielectric solvent, show that the cation radical BDEs of the lignin models are significantly lower in a highly polar media compared to the gas phase but that the relative BDEs of β-1 < β-O-4 remain the same.

Conclusions

The results obtained in this study pertain to several features of the oxidative cleavage reactions of lignin model compounds. The nature and kinetics of C−C bond cleavage reactions of cation radicals, produced from the diastereomeric β-1 and β-O-4 model compounds by using SET-sensitized photochemical and Ce(IV)-promoted oxidative processes, have been elucidated. In addition, lignin peroxidase catalyzed reactions of the model compounds were explored in order to determine product distributions and kinetic parameters. The results show that a significant difference exists between the rates of cation radical C−C bond cleavage reactions of the β-1 and β-O-4 structural units found in lignins, with cation radicals of the β-1 models undergoing this process much more rapidly than those of the β-O-4 compounds. The close agreement between the results of the quantum mechanical calculations and the experimental findings serves to validate the use of the calculations as a predictive tool for more complex lignin compounds, an issue that will be addressed in future studies. The observations made in this effort have potential relevance to the field of cellulosics research since they might provide insight into the selection and genetic design of plants that have the types of lignin structures that lead to optimal efficiencies of SET-promoted enzymatic delignification and, consequently, that are most promising for ethanol production.

Experimental Section

General. All reagents were obtained from commercial sources and used without further purification, and solvents were dried using standard procedures. ^{1}H and ^{13}C NMR (500 MHz) spectra were recorded on $CDCl_3$ solutions, and the chemical shifts of resonances are reported in parts per million relative to $CHCl_3$ (7.24 ppm) serving as an internal standard. HRMS data were obtained by using electrospray ionization or fast atom bombardment. Photochemical reactions were conducted with an apparatus consisting of a 450 W Hanovia medium vapor pressure mercury lamp surrounded by a uranium glass filter in water-cooled quartz immersion well and quartz glass tubes containing solutions of substrates in a merry-go-round photoreactor. All products were isolated as oils unless otherwise specified, and the purity of each was determined to be >90% by ^{1}H and ^{13}C NMR analysis. Column chromatography was performed using 230−400 mesh silica gel. Identification of products from photochemical, metal oxidation, and enzymatic reactions were identified by comparing their spectroscopic and chromatographic properties with those of independently synthesized or commercially available compounds. Product yields were obtained by using HPLC analysis (a 4.6 mm diameter Restek Ultra Aqueous C-18 reverse phase column with pore size 5 μm and a MeOH/H_2O gradient) based on calibration curves constructed by using known or synthesized substances.

Synthesis of *threo*-1-(4-Hydroxy-3-methoxyphenyl)-2-(3,4-dimethoxyphenyl)-1,3-diol Acetonide (15T). 4-Benzoyloxy-3-methoxybenzaldehyde (13). To a solution of vanillin (20.0 g, 120.4 mmol) in 300 mL of MeCN containing K_2CO_3 (20.0 g, 153 mmol) was added benzoyl chloride (22.0 g, 156.5 mmol). The resulting solution was stirred at 90 °C for 15 h and filtered, and the filtrate was concentrated in vacuo to give residue, which was extracted with EtOAc and 5% $NaHCO_3$. The organic extracts were dried and concentrated in vacuo, gving a solid residue that was crystallized from diethyl ether to yield the known[96] aldehyde **13** (22.8 g, 70%). ^{1}H NMR 3.87 (s, 3H), 7.34 (d, 1H, J = 7.5 Hz), 7.49−7.53 (m, 4H), 7.64 (t, 1H, J = 7.5 Hz), 8.20 (d, 2H, J = 8.5 Hz), 9.96 (s, 1H).

Diastereomeric Ethyl 1-(4-Benzoyloxy-3-methoxyphenyl)-2-(3,4-dimethoxy phenyl)acetates (14E and 14T). A solution of diisopropylamine (4.6 mL, 32.8 mmol) in dry THF (30 mL) containing 13.1 mL (32.8 mmol) of 2.5 M *n*BuLi at −78 °C was stirred for 30 min. Acetate ester **9** (7.4 g, 32.8 mmol) was added dropwise, and the resulting solution was stirred for 1 h, followed by addition of aldehyde **13** (7.0 g, 27.3 mmol). After 3 h of additional stirring at the same temperature, the mixture was diluted with H_2O and extracted with EtOAc. The organic layer was dried and concentrated in vacuo to give a residue, which was kept for 24 h at room temperature to give a solid. Rinsing the solid with diethyl ether and filtration gave **14T** (3.9 g, 30%). Concentration of the filtrate gave a residue that was subjected to column chromatography (EtOAc/hexane 1:3) to yield **14E** (2.6 g, 20%).

14T: ^{1}H NMR 1.11 (t, 3H, J = 7 Hz), 2.72 (s, 1H), 3.72 (s, 3H), 3.76 (d, 1H, J = 7 Hz,), 3.85 (s, 3H), 3.86 (s, 3H), 3.99−4.10 (m, 2H),

(96) (a) Ryckebusch, A.; Garcin, D.; Lansiaux, A.; Goossens, J.-F.; Baldeyrou, B.; Houssin, R.; Bailly, C.; Henichart, J.-P. *J. Med. Chem.* **2008**, *51* (12), 3617. (b) Kiec-Kononowicz, K.; Karolak-Wojciechowska, J.; Michalak, B.; Pekala, E.; Schumacher, B.; Muller, C. E. *Eur. J. Med. Chem.* **2004**, *39* (3), 205.

5.25 (d, 1H, $J = 7$ Hz), 6.82−6.95 (m, 5H), 7.08 (d, 1H, $J = 8$ Hz), 7.48 (t, 2H, $J = 8$ Hz), 7.61 (t, 1H, $J = 7$ Hz), 8.18 (d, 2H, $J = 7.5$ Hz, aromatic); ^{13}C NMR 13.9, 55.9, 59.1, 61.1, 74.8, 111.1, 112.1, 190.0, 121.5, 122.5, 126.8, 128.5, 129.5, 130.3, 133.4, 139.6, 139.8, 148.8, 151.1, 164.6, 172.7; HRMS (ES) m/z 503.1686 (M + Na, $C_{27}H_{28}O_8Na$ requires 503.1682).

14E: ^{1}H NMR 1.23 (t, 3H, $J = 7.00$ Hz,), 3.16 (s, 1H), 3.65 (s, 3H), 3.76 (s, 3H), 3.80 (s, 3H), 3.74 (d, 1H, $J = 7.00$ Hz), 4.15−4.26 (m, 2H), 5.12 (d, 1H, $J = 9.50$ Hz), 6.57−6.76 (m, 5H), 6.94 (d, 1H, $J = 8.50$ Hz), 7.47 (t, 2H, $J = 8.00$ Hz), 7.59 (t, 1H, $J = 7.50$ Hz), 8.15 (d, 2H, $J = 7.00$ Hz); ^{13}C NMR 14.1, 55.8, 55.9, 59.7, 61.2, 76.4, 110.7, 111.1, 111.9, 118.9, 120.7, 122.3, 127.6, 128.5, 129.4, 130.2, 133.4, 139.4, 139.9, 148.5, 148.8, 151.0, 164.5, 173.4; HRMS (ES) m/z 503.1672 (M + Na, $C_{27}H_{28}O_8Na$ requires 503.1682).

***threo*-1-(4-Hydroxy-3-methoxyphenyl)-2-(3,4-dimethoxyphenyl)-1,3-diol Acetonide (15T).** To solution of THF (60 mL) containing 1.0 M $LiAlH_4$ (22.9 mL, 22.9 mmol) was added **14T** (5.5 g, 11.4 mmol) at room temperature. After 3 h of stirring, H_2O (20 mL) and 1 N HCl (20 mL) were added at 0 °C, and the solution was extracted with CH_2Cl_2. The organic extracts were dried and concentrated in vacuo, giving a solid residue that was crystallized from diethyl ether to give the known[57m−p,97] diol (2.7 g, 70%). ^{1}H NMR 3.05 (q, 1H, $J = 6.50$ Hz), 3.74 (d, 2H, $J = 6.00$ Hz,), 3.82 (s, 3H), 3.83 (s, 3H), 3.86 (s, 6H), 4.89 (d, 1H, $J = 7.00$ Hz), 5.56 (s, 1H), 6.73−6.86 (m, 6H).

A solution of the diol (1.0 g, 3.0 mmol) in CH_2Cl_2 (40 mL) containing pyridinium *p*-toluenesulfonate (0.15 g, 0.6 mmol) and 2,2-dimethoxypropane (1.6 g, 15.0 mmol) was stirred at room temperature for 8 h and concentrated in *vauco* to give a residue that was portioned between EtOAc and satd $NaHCO_3$. The organic layer was dried and concentrated in *vacuo* to give a residue, which was subjected to column chromatography (EtOAc/hexane 1:3) to yield **15T** (0.72 g, 64%). Crystallization of the substance in 1:10 $CHCl_3$/diethyl ether gave transparent crystals of **15T**. ^{1}H NMR 1.62 (s, 3H), 1.65 (s, 3H), 3.04 (s, 3H), 3.73 (s, 3H), 3.79 (s, 3H), 3.83 (dd, 1H, $J = 14.80$ Hz, $J = 21$ Hz), 4.10 and 4.53 (two d, 2H, $J = 11.50$ Hz), 5.39 (s, 1H), 6.30 (s, 1H), 6.59−6.72 (m, 4H), 6.97 (s, 1H); ^{13}C NMR 18.8, 29.9, 45.2, 55.7, 55.8, 65.4, 73.8, 99.4, 109.3, 110.2, 113.3, 113.5, 119.0, 122.1, 132.4, 132.6, 144.5, 146.0, 147.4, 147.9; HRMS (ES) m/z 397.1627 (M + Na, $C_{21}H_{26}O_6Na$ requires 397.1630).

DCA-Sensitized Photoreactions of 8E, 8T, 4T, and 4E. General Procedure. Seventy milliliters of degassed/N_2-purged or oxgenated solutions of satd DCA (0.27 mM) in 5% H_2O/MeCN containing the substrate (1.5×10^{-5} mol, 2.1 mM) was irradiated with uranium glass filtered light for 7 h. The photolyzates were concentrated in vacuo, and the residues were subjected to HPLC analysis.

Relative Quantum Yields of DCA-Promoted Photoreactions of 4T, 4E, 8E, and 8T. Independent DCA-saturated, N_2-purged solutions, containing **4T**, **4E**, **8E**, and **8T** (1.5×10^{-5} mol, 2.1 mM) in 7 mL of 5% aqueous MeCN in quartz test tubes were simultaneously irradiated by using uranium glass filtered light in a merry-go-round apparatus for 14 h. The solutions were concentrated in vacuo, and the residues were diluted with 1.5 mL $CHCl_3$ solutions containing the standard 1,10-phenanthroline (2×10^{-3} M final concentration). Concentration of each of these solutions was followed by ^{1}H NMR analysis (peak intensities of VAD at 9.84 ppm (1H) vs 1,10-phenanthroline at 9.27 ppm (2H)) to determine the quantities of VAD formed in the photoreactions.

CAN Reactions of 4T, 4E, 8E, and 8T. Individual solutions containing the substrates **4T**, **4E**, **8E**, and **8T** (2.0 mg, 6.0×10^{-6} mol) and CAN (6.6 mg, 1.2×10^{-5} mol) in 12 mL of MeCN were stirred for 15 h at room temperature (100%, 100%, 90%, and 96% conversions of the respective substrates). The resulting mixtures were concentrated in vacuo and subjected to HPLC analysis to give the following yields. From **4T**: VAD (95%), **6** (25%), and **18** (trace); from **4E**: VAD (95%), **6** (46%), and **18** (trace); from **8E**: VAD (88%), **3** (trace), **17** (7%) and **19** (4%); from **8T**: VAD (31%), **3** (trace), **17** (32%), and **19** (33%).

19: ^{1}H NMR 3.91 (s, 3H), 3.92 (s, 3H), 3.95 (s, 3H), 4.09−4.17 (m, 2H), 5.60−5.62 (m, 1H), 6.90−6.94 (m, 2H), 7.56 (d, 1H, $J =$ 2.00 Hz), 7.69−7.71 (m, 2H), 7.92−7.94 (m, 1H); ^{13}C NMR 29.7, 56.0, 56.2, 56.4, 63.7, 83.1, 110.2, 110.8, 110.9, 111.7, 119.5, 123.4, 127.6, 141.2, 146.6, 149.5, 154.4, 155.5, 193.3; HRMS (ES) m/z 400.1008 (M + Na, $C_{18}H_{19}NO_8Na$ requires 400.1004).

CAN Reaction of 17. A 50 mL MeCN solution containing **17** (300 mg, 0.9 mol) and CAN (1.0 mg, 1.8 mmol) was stirred for 13 h at room temperature (ca. 60% conversion of **17**). The resulting mixture was concentrated in vacuo, and the residue was subjected to column chromatography to yield 187 mg (55%) of **19**.

CAN Reactivity of 4T, 4E, 8E, and 8T. The absorbances at 390 nm of independent solutions of **4T**, **4E**, **8E**, and **8T** (1.25×10^{-4} M) containing CAN (2.5×10^{-4} M) in 3.0 mL of MeCN were monitored 30 min after mixing. A plot of absorbance versus time is shown in Figure 5S (Supporting Information).

In a stopped flow apparatus, MeCN solutions of CAN (3.0×10^{-4} M) were added to solutions containing five different concentrations of **4T**, **4E**, **8E**, and **8T** (7.5×10^{-5}, 3.75×10^{-5}, 1.5×10^{-5}, 7.5×10^{-6}, 3.75×10^{-6} M). Changes in absorbances at λ_{390} (for CAN, $\lambda_{390\,nm} = 2840$) of these solutions over a 0.1−0.25 s period were monitored. From plots of time versus absorbance, initial slopes corresponding to ΔA_{390} versus t (0.1−0.25 s) of each reaction were obtained. These ΔA_{390} values were converted to concentration changes (ΔC_{lignin}), and reaction rates (v) of each reaction were determined by using the following equations: $\Delta C = \Delta A_{CAN}/\varepsilon_{390\,nm}$ and $v = \Delta C_{lignin}/0.15$. From plots of v versus concentrations (Figure 6), the rate constants (k) of CAN reaction of each compound were determined (Table 4).

In a stopped flow apparatus, MeCN solutions of **4T**, **4E**, **8E**, and **8T** (3.75×10^{-4} M) containing six different concentrations of CAN (1.5×10^{-4}, 1.8×10^{-4}, 2.1×10^{-4}, 2.4×10^{-4}, 3.0×10^{-4}, and 3.6×10^{-4} M). Changes in absorbances at λ_{390} (for CAN, $\lambda_{390\,nm}\,\varepsilon = 2840$) of these solutions over a 0.1−0.25 s period were monitored. From plots of time versus absorbance, initial slopes corresponding to ΔA_{390} versus t (0.1−0.25 s) of each reaction were obtained. These ΔA_{390} values were converted to concentration changes (ΔC_{CAN}) and reaction rates (v) of each reaction were determined by using the following equations: $\Delta C = \Delta A_{CAN}/2\varepsilon_{390\,nm}$ and $v = \Delta C_{lignin}$. From plots of v versus concentrations (Figure 5), the rate constants of CAN reaction of each compound were determined (Table 4).

Lignin Peroxidase Catalyzed Reactions of 4T, 4E, 8E, and 8T. To 0.97 mL of 0.1 M tartrate buffer (pH 3.4) were added 10 μL of each substrate **4T**, **4E**, **8E**, and **8T** (0.1 M, final concentration 200 μM) and 8 μL of H_2O_2 (1.25×10^{-2} M, final concentration 100 μM). After 15 μL of lignin peroxidase (0.15 unit, 0.36 μM) was added, the solutions were agitated for 10 min and then subjected to HPLC analysis to yield the following products from **8E** (35% conversion): VAD (35%), **3** (trace) and **17** (4%); from **8T** (66% conversion): VAD (31%), **3** (trace), and **17** (29%); from **4T** (73% conversion): VAD (52%), **5** (trace), and **6** (14%); from **4E** (77% conversion): VAD (45%), **5** (trace), and **6** (15%).

Lignin Peroxidase Reactivity of 4T, 4E, 8E, and 8T. In a stopped flow apparatus, solutions of LP (1.8 μM) in tartrate buffer (pH 3.4) containing H_2O_2 (50 μM) were mixed with solutions containing 50, 100, 150, 200, 250, 375, 500, 750, 1000, 1500, and 2500 μM of **4T**, **4E**, **8E**, and **8T**. The absorbance increases at 310 nm, corresponding to the formation of VAD and keto-alcohols **6**, **18** (for **4T** and **4E**), and **17** (for **8E** and **8T**) were measured over a 0.1−1 s time period. The ΔA_{310} values

(97) Ralph, J.; Ede, R. M.; Robinson, N. P.; Main, L. *J. Wood Chem. Technol.* **1987**, *7*, 133.

were converted to concentration changes (ΔC_{VAD}) and reaction rates (v) by using the following equations: $\Delta C_{VAD} = \Delta A/\varepsilon_{VAD,310\ nm}$ and $v = \Delta C/\text{time}$. Plots of the rates of these processes versus substrate concentration and the corresponding Lineweaver−Burk plots of $1/v$ versus 1/[S] are given in Figures S2 and S3 in the Supporting Information.

Acknowledgment. We gratefully acknowledge the support of the U.S. Department of Energy for a grant to PL (20080001DR) through the LANL/LDRD program for this work. Also, we are grateful to Taraka Dale, David Fox, and Kirk Rector at LANL for helpful discussions. R.P. acknowledges support given by the LANL Directors Postdoctoral program. U.C.Y. acknowledges support provided by the National Research Foundation of Korea Grant (2009-0072585) funded by the Korean government. Finally, we would like to thank Dr. Eileen Duesler for determining the X-ray crystallographic structure of **15T**.

Supporting Information Available: Experimental information, ^{1}H and ^{13}C NMR spectra of all previously unidentified compounds, and X-ray crystallographic data in CIF form. This material is available free of charge via the Internet at http://pubs.acs.org.